Article

Not peer-reviewed version

Bioaerosol Disinfection by a Cold Plasma Ionizer Coupled with an Electrostatic Precipitator

Wei Yang Samuel Lim , Sian Yang Ow , Sutarlie Laura * , Yeong Yuh Lee , Ady Suwardi , Ivan Tan , Wun Chet Davy Cheong , Xian Jun Loh , Xiaodi Su *

Posted Date: 31 July 2024

doi: 10.20944/preprints202407.2577.v1

Keywords: cold plasma ionizer; non-thermal plasma; electrostatic precipitator; porcine respiratory coronavirus; bacteria; bioaerosols; disinfection

Article

Bioaerosol Disinfection by a Cold Plasma Ionizer Coupled with an Electrostatic Precipitator

Samuel Wei Yang Lim, Sian Yang Ow, Laura Sutarlie *, Yeong Yuh Lee, Ady Suwardi, Chee Kiang Ivan Tan, Wun Chet Davy Cheong, Xian Jun Loh and Xiaodi Su *

Institute of Materials Research and Engineering (IMRE), Agency for Science, Technology and Research (A*STAR), 2 Fusionopolis Way, Innovis, #08-03, Singapore 138634, Republic of Singapore

* Correspondence: laura-sutarlie@imre.a-star.edu.sg (L.S.); xd-su@imre.a-star.edu.sg (X.S.)

Abstract: Despite the best efforts in air-purification, airborne infectious diseases do and will continue to spread due to continuous emission of bioaerosols by the host/infected person. To tackle the rapid spread of airborne infectious diseases, a shift in focus from air-purification to bioaerosol disinfection/ decontamination is urgently needed. In this work, we studied a cold plasma ionizer (CPI) and electrostatic precipitator (ESP)-coupled CPI (CPI-ESP) for disinfection and cleaning of bioaerosols. Using porcine respiratory coronavirus (PRCV) and *E. coli* in a testing chamber, we demonstrated that CPI coupled with ESP is an effective technology for inactivating aerosolized microorganisms and microorganisms spread on surfaces. In addition, we have demonstrated the efficiency of a CPI-ESP coupled device for disinfection of naturally occurring airborne microbials in a few indoor settings (i.e., an living room, a discussion room, a schoolroom and an office) to determine the treatment duration- and human activity-dependent efficacy. To understand the disinfection mechanism, we conduced fluorescence microscopy study to reveal different degree of bacteria cell membrane damage under CPI treatment.

Keywords: cold plasma ionizer; non-thermal plasma; electrostatic precipitator; porcine respiratory coronavirus; bacteria; bioaerosols; disinfection

1. Introduction

Bioaerosol and surface transmission are the most common routes to spread infectious respiratory diseases, for instance, the SARS-CoV-2 virus [1–3]. Reducing the spread of such infectious diseases can be achieved by either reducing human exposure to bioaerosols (e.g., wearing surgical masks) or reducing the quantity of bioaerosols via disinfection techniques.

For indoor spaces, reducing the quantity of bioaerosols can be achieved by using high efficiency particulate air filtration (HEPA filters) and electrostatic precipitator (ESP) to adsorb bioaerosols, including mold spores, bacteria, pollen, and viral particles etc. [4–7]. HEPA filters remove particles from air that are forced through, but microorganisms are known to survive on a HEPA filter [8]. On the other hand, ESP removes particles from a gas stream by using electrical energy to confer a positive or negative charge to aerial particulates [9]. The charged particles are then attracted to collector plates carrying the opposite charge. ESP is mainly used to remove particulate matter (PM) in coal-fired power plants [10,11]. It is also possible to use an ESP for antibacterial/antiviral purposes due to the generation of additional electric fields, ions and/or reactive species [12–14].

In addition to PM and bioaerosols trapping by HEPA and ESP, UV-C radiation, chemical sprays, and ionization of the air are popular approaches for bioaerosols decontamination [15,16]. Each of these technologies have their own drawbacks and application limitations. For example, direct human exposure to UV radiation is hazardous and can cause cancer and blindness. The efficiency of chemical disinfectant sprays depends on many factors, such as concentration of the chemicals, reaction time, and the presence of other organic matters that may react with the chemicals [17].

 doi:10.20944/preprints202407.2577.v1

An emerging technology for inactivation or disinfection of microorganisms is cold plasma or non-thermal plasma. Cold plasma or non-thermal plasma can be generated by the application of an electric or electromagnetic field to a gas, via various means, i.e., dielectric barrier discharge (DBD), atmospheric pressure plasma jet (APPJ), plasma needle, and plasma pencils [18,19]. The partially ionized gas is typically a mixture of excited atoms and molecules, electrons, ultraviolet photons, ions, and various other reactive species, such as singlet oxygen, ozone, hydroxyl radicals and nitrogen oxides. The various oxygen radical species (atomic oxygen, hydroxide radical, superoxide radical, HO_2, H_2O_2) and nitrogen radicals (atomic nitrogen, nitrogen oxides and peroxynitrite) are known to have excellent bactericidal effect on microbes [20], by compromising cell membranes, damaging proteins, and nucleic acids [18,21]. Cold plasma treatment has been demonstrated to be effective against bacteria [18,22,23], bacterial endospores [24,25], microbial toxins [24], fungi [26], and viruses [19,26–28] in various disinfection applications, including food production [24,29,30], wound healing [31], and medical device sterilization [32,33]. Cold plasma technology can also be used to disinfect N95 masks to allow for safe re-use of the mask [34], and reducing the environmental impact from widespread use of masks.

When faced with disinfection techniques, microorganisms tend to develop a resistance to the particular techniques due to selective pressures [29]. In the case of cold plasma, an upregulation of catalase or redox-active chemical production in bacteria could cause the bacteria to develop a tolerance towards cold plasma exposure [18,35]. As such, a combined disinfection method would be more effective at preventing the development of resistance towards airborne disinfection.

In this study, we systematically studied a dielectric barrier discharge (DBD) type cold plasma ionizer (CPI) for its efficiency to inactivate bacteria (using *E. coli* as the model organism) and virus (using porcine respiratory coronavirus (PRCV) as a surrogate for SARS-CoV-2), without and with coupling to an electrostatic precipitator (ESP). We firstly studied the capability of a CPI and a CPI coupled with an ESP (CPI-ESP) to disinfect/inactivate bacteria/virus on surfaces (without aerosolization) and then for *E. coli* aerosolized in air using a nebulizer. A testing chamber was built to host the bacteria samples, CPI-ESP coupled apparatus, PM (particulate matter) meters, a particle analyzer, an ozone meter, and the nebulizer. For air disinfection studies, the chamber is further equipped with a liquid impinger air sampler to collect the aerosolized *E. coli* before and after CPI or CPI-ESP treatment. Following the study in the test chamber, we demonstrate the efficiency for general bacteria disinfection in various air-conditioned indoor settings, i.e., an office room, a living room, a large discussion room, and a school room. In addition, we have demonstrated the treatment duration- and human activities-dependent disinfection efficacy of a commercial CPI-ESP equipment. To understand the disinfection mechanism and address the safety concerns, we monitored the ozone level in the chamber and in an office room (one of the air-conditioned indoor settings studied). With this study, we demonstrated that the CPI- ESP is an effective and safe tool for bioaerosol disinfection.

2. Materials and Methods

2.1. Biological Agents and Cultivation Processes

Porcine respiratory coronavirus (PRCV) was purchased from ATCC (CRL-2384). The virus was propagated in ST cells (ATCC CRL-1746) grown on Minimum Essential Medium (MEM) containing 2 mM glutamine and Earle's balanced salts (Cytiva), with addition of 1 mM sodium pyruvate (Lonza), 1× MEM Non-essential Amino Acid Solution (Sigma) and 2% fetal bovine serum (Gibco) according to ATCC's growth conditions. The virus was separated from host cells by centrifugation after observed cytopathic effects and stored in stock solution aliquots under -80 °C. The concentration of PRCV in the stock solution aliquots was determined by Median Tissue Culture Infectious Dose ($TCID_{50}$) assay to be 6.95×10^8 $TCID_{50}$/mL, taking an average of the estimated viral concentration as calculated by the Reed-Muench method and the improved Kärber method. PRCV was stored in the ATCC recommended Viral Media, which consists of MEM supplemented with ~1 mM sodium pyruvate and 1× non-essential amino acids.

Escherichia coli (*E. coli*) strain ATCC 25922 was purchased from ATCC and grown on nutrient agar (Oxoid) in an incubator for 24 h at 37 °C. To prepare a working culture, freshly cultured colonies

 doi:10.20944/preprints202407.2577.v1

of *E. coli* were suspended in sterile 0.9% NaCl or 1× PBS Phosphate Buffered Saline (PBS). The suspensions were diluted to an optical density at 600 nm (OD_{600}) value of 0.25, which corresponds to 1-2 × 10^8 CFU/mL. A plate count was performed post experiment to determine the actual bacteria concentration.

2.2. Apparatus and Testing Chamber

An in-house built CPI coupled with an ESP was prepared by modification of an air disinfection system procured from EddaAir (China). The CPI tube (in the EddaAir device) is 180 mm long with power specifications of 12 VDC and 50 W. The air volume sampling rate is 138m^3/h. For the purpose of this study, other air purification/ disinfection components in this system (HEPA filters and a UV lamp) were replaced with an improvised ESP component comprising of a discharge electrode and metal collector according to the work by Suwardi et.al. [36] as shown in Figure 1. During this study, the power input and fan speed was not changed. Hence, the plasma-induced ROS and RNS generation profiles and air flow rate were presumed to be fixed based on the specifications of the EddaAir product.

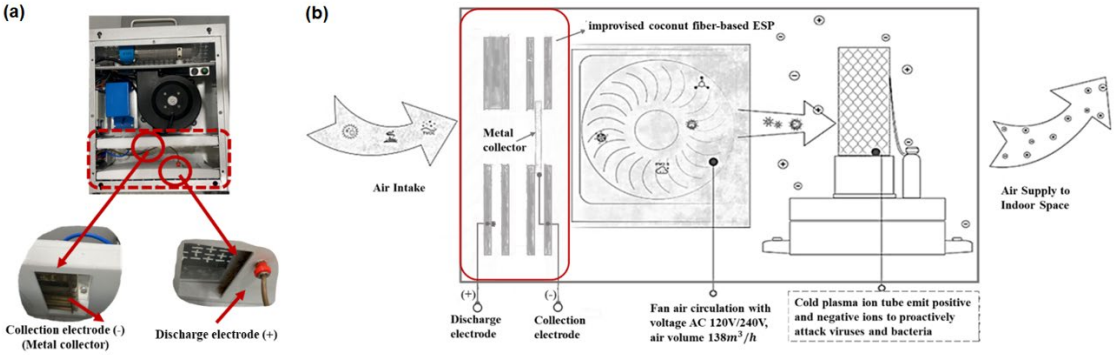

Figure 1. (**a**) In-house built CPI-ESP from partially modified EddaAir cold plasma device, (**b**) schematic drawing of the components inside the CPI-ESP.

This modified CPI-ESP device was used for all experiments related to lab strain-virus and -bacteria that were performed in an in-house built closed acrylic chamber (75 × 44 × 47 cm with a total volume of 155 L) placed in a sterile biosafety cabinet illustrated in Figure 2. The CPI and ESP are modular and can be operated separately. The ESP component was turned off when the CPI effect was studied. Both the CPI and ESP components were turned on when studying the coupled CPI-ESP effect.

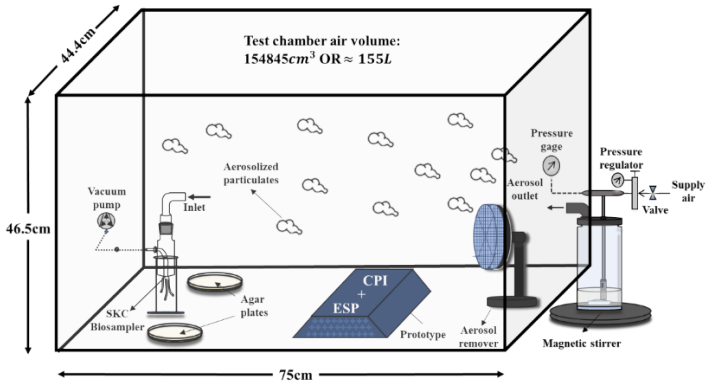

Figure 2. Schematic drawing of the bioaerosol testing chamber and the apparatus components.

 doi:10.20944/preprints202407.2577.v1

A commercial air disinfection system (Plasma Science Pte. Ltd., Singapore) containing similar coupling of a CPI with an ESP was deployed for air disinfection study in various indoor settings. This commercial system integrated a CPI tube with an ESP apparatus that consists of a paired collection and discharge electrode plates. The specified clean air delivery rate (CADR) was set at 400 m^3/h. Ozone concentration was monitored using an Indoor Air Quality (IAQ) certified tool (Model: Aeroqual Series 500).

2.3. Inactivation of Porcine Respiratory Coronavirus Droplets on Surfaces

Porcine respiratory coronavirus (PRCV) spread on glass coverslips and/or *E. coli* agar plates were placed in the chamber close to the CPI-ESP device. Glass coverslips were sterilized via 10 minutes UV irradiation on both sides in a biosafety cabinet (BSC) hood using the UV lamp. In the bioaerosol chamber, virus solution (10 µL) was spread as ten microdroplets on a sterile glass coverslip (two duplicate coverslips in each experiment repeated twice). The CPI-ESP device in the chamber was then turned on for different durations of exposure time (from 5 to 60 minutes). After the desired exposure time, the virus samples were then taken out from the chamber and recovered by the addition of 1 mL of viral media to the glass coverslip and the virus was resuspended via pipetting. The concentration of live virus in the collected viral media from each sample was analyzed via a $TCID_{50}$ assay. The same amount of virus solution spread on a glass slide but not exposed to CPI or CPI-ESP was used as a negative control. The live virus titer in the control and after inactivation treatment was calculated after 5 days observation. Where no cytopathic cells were observed in any of the treated wells, we assumed the final viral titer as 6.31 $TCID_{50}$/mL which is the estimated limit of detection of such assays [37]. The disinfection efficiency was calculated as percentage reduction of live virus after exposure to CPI or CPI-ESP treatment, relative to the control by formula (1):

$$Percentage\ reduction\ (\%) = \frac{TCID_{50}{}^{Control} - TCID_{50}{}^{CPI\ (CPI-ESP)}}{TCID_{50}{}^{Control}} \times 100 \quad (1)$$

2.4. Disinfection of Bacteria on Surfaces

In the testing chamber, 100 µL of 10^4 to 10^3 CFU/mL *E. coli* suspended in sterile 0.9 % NaCl was spread on agar plates using an L-spreader (2 duplicates) and placed at a proximate distance from the CPI (or CPI-ESP) inside the chamber. The disinfection apparatus was turned on for various exposure time (5 to 60 minutes). After exposure, the agar plates were removed for incubation at 37°C in an incubator overnight. The same bacteria batch spread on separate agar plates not exposed to CPI or CPI-ESP were used as negative control. The number of bacteria colonies on the agar plates was counted after overnight incubation. This experiment was repeated at least twice for each time point. The disinfection efficiency was calculated as percentage reduction of colony forming units (CFU) left on the plate after exposure to treatment relative to the control by the following formula (**2**):

$$Percentage\ reduction\ (\%) = \frac{CFU^{Control} - CFU^{CPI\ (CPI-ESP)}}{CFU^{Control}} \times 100 \quad (2)$$

2.5. Aerosolization of Bacteria and Bioaerosol Disinfection Study

Prior to the bioaerosol disinfection study, the aerosolization of *E. coli* in the testing chamber was optimized and characterized. A Collison Nebulizer (CH Technologies, USA) was used to generate bioaerosols from *E. coli* solution (75 mL of 10^6 or 10^5 CFU/mL *E. coli* in sterile 1× PBS). Particulate sensors (Sensirion SPS30) were placed in the chamber to characterize the generated bioaerosol particle concentration and size profile, with real-time data sent wirelessly to a computer. The sensors were calibrated using TSI DustTrakTM DRX Aerosol Monitor 8533 as a reference. The particle concentration and size profiles of aerosolized *E. coli* generated by the nebulizer at various air pressure was shown in Figure S1. The distribution of the *E. coli* across the testing chamber was characterized by passive agar sampling placed on various spots in the chamber (Figure S2a) to determine the positioning of a liquid impinger air sampler (BioSampler from SKC Inc.) for an active bioaerosol sampling. Based on the characterization results (Figure S2b-e), the optimized positioning of the SKC Biosampler for the bioaerosol disinfection experiment was determined at the opposite far end of the

 doi:10.20944/preprints202407.2577.v1

nebulizer, along the center line. In the bioaerosol disinfection experiment, the nebulizer was turned on for a total of 20 minutes, while at the 5 minutes timepoint the SKC BioSampler was turned on for 30 minutes. The SKC BioSampler was filled with 20 mL of sterile 1× PBS for collection of the *E. coli* bioaerosols and operated with pump at a flow rate of 12.5 L/minute. Two nutrient agar plates were placed on each side of the SKC BioSampler and are equally spaced apart to account for the settlement of bioaerosols (as a passive sampler). The CPI device was started either prior to the nebulizer, allowing the test chamber to be saturated with CPI emissions or at the same time as the nebulizer was turned on. At the end of the disinfection experiments, the collection media from the SKC BioSampler was retrieved. Then 100 μL of the collection media was spread onto nutrient agar plates in duplicates. The passive agar collection plates were also retrieved from the test chamber and incubated for 24 hours at 37°C before the number of bacteria colonies on each plate was counted.

2.6. Fluorescence Microscopy Studies of E. coli Samples

Fluorescence microscopy studies were conducted using a Leica DM5000B microscope and an improved Neubauer cell counting slide using 10× magnification. Before viewing under microscope, 10 μL of sample was mixed with 10 μL of Baclight™ viability assay stain and incubated for 5 minutes. Five separate images were obtained by using the GFP (Excitation of 430-510 nm, Emission of 475-575 nm) filter and N21 (Excitation of 515-560 nm, Emission of 590 nm) filter. The stain is a mixture of two DNA-binding fluorescent dyes: SYTO9 and propidium iodide (PI). The former is used to identify all bacteria and the latter to identify bacteria with a compromised cell membrane (i.e., dead cells) [38]. Total bacteria (live and dead) were estimated by counting the number of fluorescent particles observed in the GFP filter, which are SYTO9 dye-stained cells. Then the dead bacteria were estimated by counting the number of fluorescent particles under the N21 filter, which are PI-stained dead cells.

2.7. Bioaerosol Disinfection Studies in Indoor Settings

The bioaerosol disinfection studies by using CPI-ESP in indoor setting were performed in indoor air-conditioned public spaces with a commercial CPI-ESP equipment (Airdome™70, Plasma Science Pte. Ltd., Singapore). The commercial CPI-ESP equipment has a clean air delivery rate (CADR) of up to 400 m^3/h that mimics open air factor (OAF) condition [39,40] by generating reactive species during air ionization and delivering revitalized clean air.

With concerns related to ozone generation by CPI, we performed ozone monitoring measurements without and with the commercial CPI-ESP equipment in a meeting room of 32.5 m^3 volume space. Each monitoring test runs for a duration of 8-hours referenced to the guidelines by National Environmental Agency (NEA), Singapore. Before and after CPI-ESP treatment, air sampling was performed by using the nutrient agar-based FKC-III microbial air sampler, which was operated for 20 minutes with a flow rate of 100 L/minute. All agar plates were incubated at 37°C in an incubator for 5 days before the various bacteria and fungi colonies were counted. The Aerotrak™ particle counter was also operated with a flow rate of 2.83 L/minute for the same duration of 20 minutes, to count 1 μm particulate matters. We have conducted studies on two indoor settings. The first one was to investigate the effect of CPI-ESP treatment duration on air cleaning and air disinfection efficacy. This study was carried out in a living room and a discussion room with a similar volume space of 60 m^3. The commercial CPI-ESP coupled air purifier was operated for 1 hour and 24 hours, respectively. Secondly, to investigate the effect of human activity inside the room to the air cleaning and air disinfection efficacy, a schoolroom with human activity and an office with no human activity were assessed. Both settings had similar volume space of 375 m^3.

3. Results and Discussion

3.1. Inactivation of Virus and Bacteria on Surfaces

We first studied the capability of CPI and the combination of CPI-ESP to inactivate virus (PRCV) and bacteria (*E. coli*) on surfaces without aerosolization in a testing chamber. The operational principle and design of the CPI and ESP is illustrated in Figure 3. The CPI generates reactive oxygen

 doi:10.20944/preprints202407.2577.v1

and/or nitrogen species responsible for virus inactivation through effects on capsid proteins and/or nucleic acids (Figure 3a) [28]. ESP is a platform that can attract microbial particles by electrostatic interactions [39]. The ESP used in this study is a two-stage precipitator where the charging field and the collecting field are independent of each other. Corona discharge occurring in the ESP illustrated in Figure 3b may contribute to the total amount of disinfection species emitted by the combined CPI-ESP device.

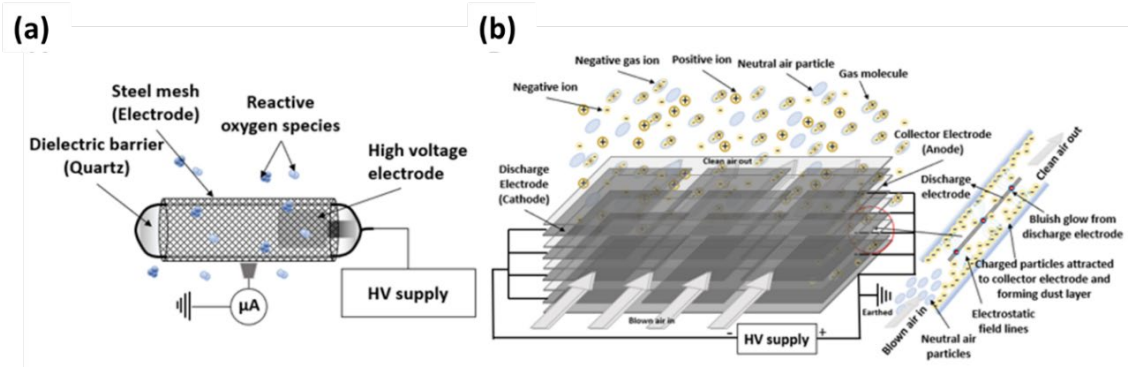

Figure 3. Schematics of (**a**) Dielectric Barrier Discharge (DBD)-based CPI and (**b**) ESP.

The disinfection outcomes by the CPI device and the integrated CPI-ESP device were plotted as percentage of reduction in number of microbial as a function of treatment time (Figure 4). For *E. coli*, the integrated CPI-ESP device was able to inactivate at least 99.9% of the bacteria within 5 minutes of exposure, whereas by CPI alone, 30 minutes was needed to achieve the same degree of reduction shown in Figure 4a. For PRCV, 99.8% inactivation was achieved in 15 minutes by the CPI-ESP device, whereas the CPI alone only achieved ~60% inactivation for the same 15 minutes treatment shown in Figure 4b. At 30 minutes treatment, 99.99% reduction (4 log) was achieved by the CPI-ESP, whereas that by CPI was only 99.8% (~ 3 log). For both *E. coli* and PRCV, the coupled CPI-ESP device shows higher inactivation efficiency than CPI alone. While the ESP component is expected to be more effective against bioaerosols as a precipitator for bioaerosols, the higher disinfection efficiency shown by the combined CPI-ESP device for the *E. coli* and PRCV on surfaces could be due to the generation of additional electric fields, ions, or reactive species from the ESP device [12–14,39] that attacked the bacteria and virus on the surface.

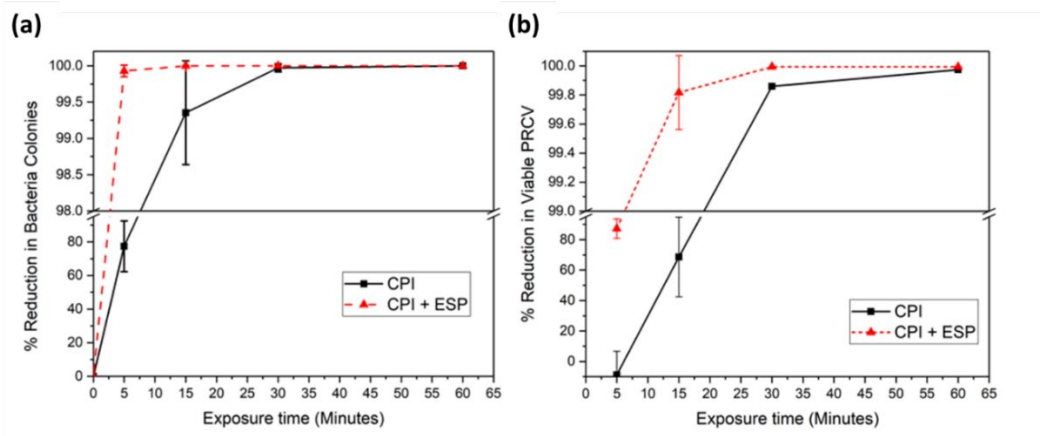

Figure 4. Percentage reduction of (**a**) *E. coli* and (**b**) PRCV in the testing chamber over time. The standard deviations at 5-minute and 15-minute are 6.43% and 0.25%, respectively. The standard deviations beyond 30-minute remained as zero from no viable counts.

Preprints.org (www.preprints.org) | NOT PEER-REVIEWED | Posted: 31 July 2024 doi:10.20944/preprints202407.2577.v1

When comparing results between the PRCV and *E. coli* shown in Figure 4, our data shows that *E. coli* is more susceptible to CPI (and CPI-ESP) inactivation than PRCV. For CPI treatment of 15 minutes, for example, over 99% of the *E. coli* was killed, as compared to PRCV that was only inactivated by about 60%. Similarly, under the CPI-ESP treatment, in 5 minutes the *E. coli* was inactivated up to 99.9%, but PRCV needs 15 minutes to reach to similar degree of inactivation (99.8%). In an earlier study of UV disinfection of *E. coli* and MS2 bacteriophage (an icosahedral, positive-sense single-stranded RNA virus), the higher susceptibility *E. coli* to UV disinfection than MS2 was observed as well [33]. The relatively strong resilience of virus than bacteria has been observed in other disinfection methods by UV of other biocides that structural damage to viral capsids and even to DNA polymerases may not always result in the loss of infectivity of the virus [40].

3.2. E. coli Bioaerosol Disinfection in the Testing Chamber

To study the disinfection of bioaerosols, *E. coli* was aerosolized by using a nebulizer and sampled by passive sampling using agar plates and active sampling using a liquid impinger (SKC BioSampler). The timeline for the operation of the CPI, nebulizer and SKC BioSampler was shown in the timeline (Figure 5a) with two CPI operation arrangements. For both arrangements, the nebulizer and SKC BioSampler were operated at duration of 20 minutes and 30 minutes, respectively, and the BioSampler was turned on at 5 minutes into the operation of the nebulizer. The CPI treatment started either earlier prior to the nebulizer to allow ion saturation within the chamber (arrangement 1); or started at the same time as the nebulizer (arrangement 2). To study the CPI disinfection efficiency over time, the CPI device was run at desired durations of 5, 15, or 30 minutes to generate different ions concentration. For arrangement 1, the CPI device was kept on for ~45 min before turning on the nebulizer for consistency.

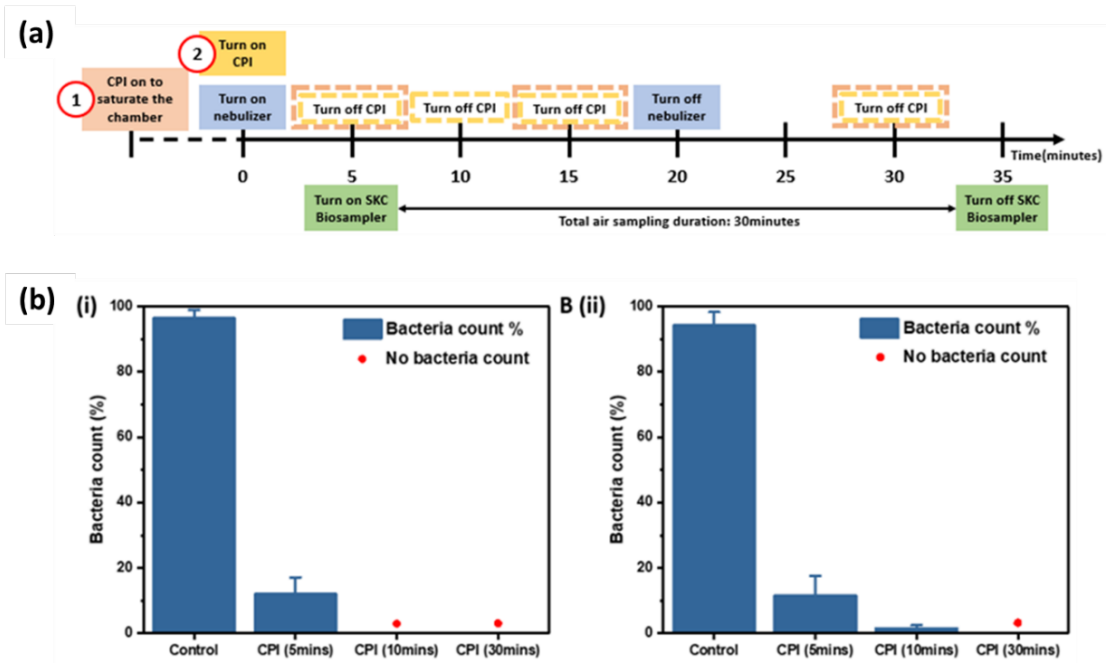

Figure 5. (**a**) Timelines illustrating the operational sequence of the nebulizer, SKC BioSampler and the CPI device for air disinfection study. The CPI operation was in two arrangements 1 and 2. (**b**) CPI disinfection of aerosolized *E. coli* with CPI operational timeline arrangement 2, using (**i**) active sampling by SKC BioSampler and (**ii**) passive sampling on agar plate.

The effectiveness of the CPI device to inactivate aerosolized *E. coli* with CPI operation arrangement 1 and 2 were determined over time. In CPI operational timeline arrangement 1, when the chamber is filled with ions, no bacteria colonies were grown from SKC collection liquid, nor on the passive sampling agar plates as short as 5 minutes treatment. From CPI operation arrangement

 doi:10.20944/preprints202407.2577.v1

1, the control *E. coli* count without CPI treatment was ~200 and ~3,000 CFU/mL, from SKC collection liquid and passive agar sampling, respectively (Figure S3). Therefore, at least 2 log reduction (> 99%) of viable bacteria from the SKC sampling and 3 log (> 99.9%) reduction of viable bacteria from the passive sampling were achieved. To further verify the deactivation and killing effect of cold plasma ions at different time when the chamber is not pre-saturated, the CPI and nebulizer were turned on together (CPI operational timeline arrangement 2). The bacteria count results are in supporting information, Figure S4. As expected, a longer duration of at least 10 minutes is needed to reach to the respective 99% and 99.9% reduction of viable bacteria from the two sampling methods as shown in Figure 5b.

In comparison to inactivation of *E. coli* on surfaces, where 99.9% reduction was achieved after 30 min exposure to CPI, the *E. coli* bioaerosol inactivation reached to 99.9% at a faster time of only 10 minutes of CPI exposure. Such faster disinfection by the CPI treatment to bioaerosols could be due to the significantly higher contact area of aerosolized particles to CPI disinfection species, while the bacteria on surfaces are only partially exposed to the atmospheric CPI disinfection species.

3.3. Fluorescence Microscopy Study of Bacteria Death in Bioaerosols

To uncover the disinfection mechanism and effect of atmospheric CPI disinfection species on the *E. coli* bioaerosols, fluorescence microscopy characterization of the liquid collected from the SKC BioSampler with and without CPI treatment was performed using SYTO9 and PI dyes. The SYTO9 dye is permeable to cell membranes so it stains both live and dead biological particles or cells; whereas PI dye is unable penetrate intact cell membranes so it can only stain biological particles with compromised cell membrane, i.e., dead cells [38,42]. Figure 6 shows the ratio of dead cells to total cells (live and dead) with and without CPI treatment following operational timeline arrangement 1 (saturated CPI, Figure 6a.) and arrangement 2 (un-saturated CPI, Figure 6b).

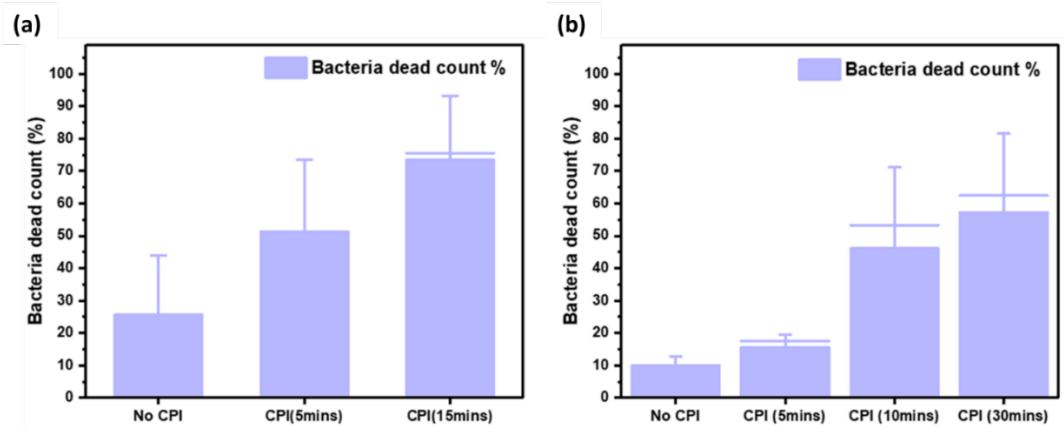

Figure 6. Average percentage of dead bacteria from fluorescence microscopy counting. Error bars represent the standard deviation. (**a**) CPI treatment starting at the beginning of the experiment in CPI as-saturated test chamber (**b**) CPI treatment starting at the beginning of the experiment.

In the absence of CPI, about 10% to 27% of the collected bacteria are dead as confirmed by PI fluorescence indicating damaged membrane (Figure S5). When CPI is operated, the proportion of the dead cells increased in a time dependent manner. There was a presence of "live" cells that have intact membranes as confirmed by the fluorescence microscopy with the SYTO9/PI staining (Figure S6-S7), despite the absence of bacteria colonies from plate counts of the same SKC collection liquid. This indicates that the bacteria may have entered a "viable but not cultivable" state or may have otherwise been rendered non-viable without membrane perforation from the CPI treatment. Both the states are likely a result of damage to various cell surface components. Additionally, the presence of more dead bacteria with membrane perforation at a higher exposure time suggests that the cumulative damage from longer CPI exposure eventually results in membrane integrity failure and cell death.

 doi:10.20944/preprints202407.2577.v1

The presence of fluorescent bacteria in the fluorescence microscopy studies also shows that CPI exposure under these conditions does not significantly break up DNA, as both SYTO9 and PI are DNA intercalating dyes.

When comparing between the two CPI operational arrangements, within 5 minutes, there was a much larger proportion of dead cells (52%) for the saturated CPI operation as compared to non-saturated operation (15%). This indicates that the viable bacteria concentration decreased with longer CPI saturation conditions. Studies in a review by Zhang et al. on bactericidal properties of cold plasma have explained the bacteria inhibition mechanisms [43]. The actions of ROS and RNS species generated by CPI including oxidation and perforation of cell membrane, degradation and modification of proteins, and modification and chain-breaking of nucleic acid molecules. Since we used *E. coli*, a gram-negative bacillus with a thin peptidoglycan cell wall in this study, plasma-induced reactive species should mainly damage the cells via membrane peroxidation, thus inducing leakage of intracellular material [44].

3.4. Air Disinfection in Indoor Room Settings

Moving from the experimentally aerosolized *E. coli* in the test chamber to naturally occurring airborne microorganisms in indoor room settings, we investigated the effect of treatment duration and human activity to bioaerosols disinfection efficacy by using a commercial CPI-ESP setup in indoor public spaces, i.e., a living room, a discussion room, a schoolroom, and an office. Prior to the bioaerosol disinfection study in indoor settings, we conducted ozone monitoring over a period of 8 hours in 10-minute intervals without and with the commercial CPI-ESP setup to determine if the ozone level is within the safe limit based on safety guidelines by NEA, Singapore. The ozone monitoring results show that the operation of the commercial CPI-ESP setup did not lead to significant increase in the ozone level, with which within the safety limits of 0.05 ppm (Figure S8).

Upon safety confirmation, we then determined the treatment duration dependent inactivation efficacy in two indoor settings of similar room volume of 54 m^3, i.e., a living room and a discussion room. Results (Figure 7a) show that 528 CFU and 529 CFU of bacteria were collected prior to the CPI-ESP treatment from the living room and discussion room, respectively, while only 119 CFU and 50 CFU of bacteria were collected from the living room with 1 hour of CPI-ESP treatment and the discussion room with 24 hours of CPI-ESP treatment, respectively. The inactivation efficacy in terms of percentage from 24 hours of treatment (90.5%) is higher than the 1 hour of treatment (77.5%), as expected. We also measured the indoor air PM concentration (Figure 7b). An average of 726 and 137 particle counts in 20 minutes sampling time were observed in the absence of CPI-ESP treatment, while only 279 and 23 particle counts were observed with CPI-ESP treatment from the living room and discussion room, respectively. Coherent with the viable count results, higher air cleaning efficacy (83.2%) is observed from the particle count results after 24 hours of treatment which is better than 1 hour of treatment (61.6%). The effectiveness of CPI-ESP systems against naturally occurring airborne microorganisms and airborne particulates, and the treatment time dependency are confirmed.

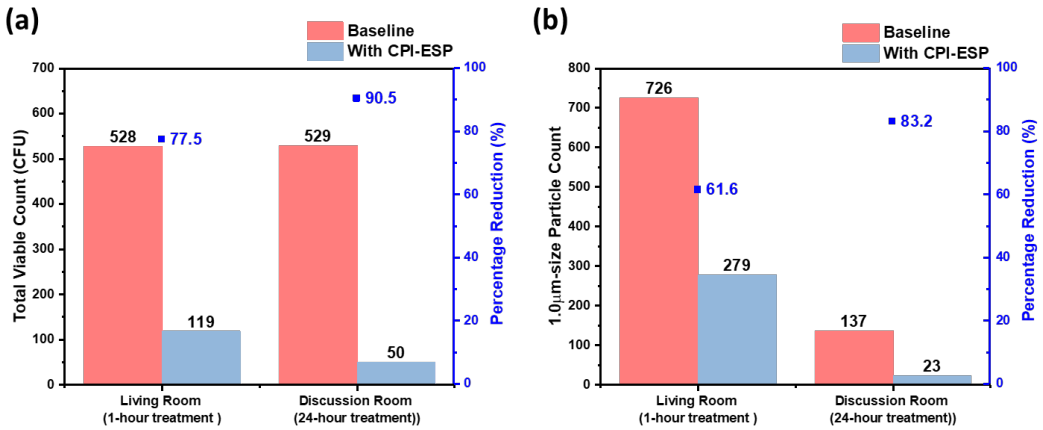

 doi:10.20944/preprints202407.2577.v1

Figure 7. (**a**) Total viable count (N=1) and (**b**) 1 μm-size particle count results (N=1) from a living room and a discussion room of similar room volume for 1-hour and 24-hour treatment by a commercial CPI-ESP equipment.

Next, to study the effectiveness of CPI-ESP bioaerosol disinfection in settings with and without human activities, the commercial CPI-ESP equipment was placed in two other public indoor spaces, i.e., a schoolroom and an office of similar space volume of 375 m^3. In the schoolroom, there were at least 40 children playing and having lessons, while there was no human activity in the office. In both settings, the treatment time was set as 1 hr. Figure 8a shows that 1672 CFU and 214 CFU of bacteria were collected from the schoolroom and office in the absence of CPI-ESP treatment, respectively, while only 676 CFU and 42 CFU of bacteria were collected after the treatment. The inactivation efficacy (in terms of percentage) for the schoolroom (59.6%) is lower than that for the empty office (80.4%). Similar as the viable count results, the particle count results (Figure 8b) showed a lesser air cleaning efficacy in the schoolroom (23.5%) as compared to the empty office (69.7%). This is due to the fact that human activities can continuously generate viable bioaerosols. Hence, the operation of the CPI-ESP (duration and/or timeframe) should be designed according to the real case scenarios.

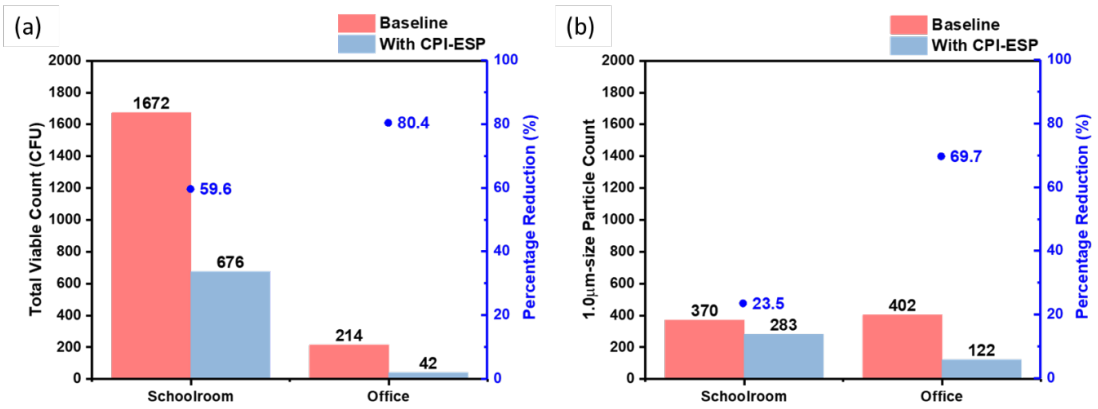

Figure 8. (**a**) Total viable count (N=1) and (**b**) 1µm-size particle count results (N=1) for a schoolroom and an office with and without on-going human activities, respectively after 1-hour treatment by a commercial CPI-ESP equipment.

4. Conclusion

In this study we have studied a CPI and a ESP coupled CPI (CPI-ESP) devices for bioaerosols disinfection. Through experiments in a controlled testing chamber, we have demonstrated that the CPI-ESP combination is more effective in the inactivation of virus and bacteria than CPI alone. **Furthermore, the reduction of** aerosolized viable microorganism by the CPI-ESP device is faster than the reduction of surface spread microorganism. We have also exploited a commercial air purifier with CPI coupled ESP to study the disinfection in indoor settings with and without human activities. The results showed that the CPI-ESP system is effective in reducing the quantity of viable naturally occurring environmental microorganisms, in a treatment time-dependent manner; and even in the presence of human activities. Furthermore, we observed that CPI treatment would result in bacteria becoming non-viable before death by membrane perforation using fluorescence microscopic techniques. The experimental demonstration and understanding derived from this work can enhance the understanding of the mechanism of air disinfection by CPI-ESP and provide guidance for future optimization of this combined technologies.

Supplementary Materials: The following supporting information can be downloaded at the website of this paper posted on Preprints.org.

 doi:10.20944/preprints202407.2577.v1

Author Contributions: Samuel Wei Yang Lim: Conceptualization, Methodology, Data curation, Investigation, Writing- Original draft preparation and drawing. **Sian Yang Ow:** Conceptualization, Methodology, Data curation, Investigation, Writing- Original draft preparation. **Laura Sutarlie:** Conceptualization, Data Curation, Investigation, Writing-Reviewing and Editing. **Yeong Yuh Lee:** Data curation, Investigation, Writing-Reviewing and Editing. **Ady Suwardi:** Conceptualization, Supervision, Methodology, Writing-Reviewing and Editing. **Chee Kiang Ivan Tan:** Conceptualization, Supervision, Writing-Reviewing and Editing. **Wun Chet Davy Cheong:** Supervision, Conceptualization, Writing-Reviewing and Editing. **Xiaodi Su:** Funding Acquisition, Supervision, Project Administration, Writing-Reviewing and Editing. **Xian Jun Loh:** Conceptualization, Supervision, Writing-Reviewing and Editing.

Data Availability Statement: Data will be made available on request.

Acknowledgments: This project was supported by The National Centre for Infectious Diseases (*NCID*), Singapore [PREPARE-CS1-2022-003].

Conflicts of Interest: The authors declare that they have no known competing financial interests or personal relationships that could have appeared to influence the work reported in this paper.

References

1. Lotfi, M., M.R. Hamblin, and N. Rezaei, *COVID-19: Transmission, prevention, and potential therapeutic opportunities.* Clinica Chimica Acta, 2020. **508**: p. 254-266.
2. Lewis, D., *Why indoor spaces are still prime COVID hotspots.* Nature, 2021. **592**(7852): p. 22-25.
3. Yao, M., *SARS-CoV-2 aerosol transmission and detection.* Eco-Environment & Health, 2022. **1**(1): p. 3-10.
4. Gavahian, M., C. Sarangapani, and N.N. Misra, *Cold plasma for mitigating agrochemical and pesticide residue in food and water: Similarities with ozone and ultraviolet technologies.* Food Research International, 2021. **141**: p. 110138.
5. Misra, N.N. and A. Martynenko, *Multipin dielectric barrier discharge for drying of foods and biomaterials.* Innovative Food Science & Emerging Technologies, 2021. **70**: p. 102672.
6. Vijayan, V.K., et al., *Enhancing indoor air quality -The air filter advantage.* Lung India, 2015. **32**(5): p. 473-9.
7. Berry, G., et al., *A review of methods to reduce the probability of the airborne spread of COVID-19 in ventilation systems and enclosed spaces.* Environmental Research, 2022. **203**: p. 111765.
8. Mittal, H., et al., *Survival of Microorganisms on HEPA Filters.* Applied Biosafety, 2011. **16**(3): p. 163-166.
9. Pirhadi, M., A. Mousavi, and C. Sioutas, *Evaluation of a high flow rate electrostatic precipitator (ESP) as a particulate matter (PM) collector for toxicity studies.* Science of the Total Environment, 2020. **739**: p. 140060.
10. Zheng, C., et al., *A real-time optimization method for economic and effective operation of electrostatic precipitators.* Journal of the Air & Waste Management Association, 2020. **70**(7): p. 708-720.
11. Sudrajad, A. and A.F. Yusof, *Review of electrostatic precipitator device for reduce of diesel engine particulate matter.* Energy Procedia, 2015. **68**: p. 370-380.
12. Feng, Z., et al., *Indoor airborne disinfection with electrostatic disinfector (ESD): Numerical simulations of ESD performance and reduction of computing time.* Building and Environment, 2021. **200**: p. 107956.
13. Viner, A.S., et al., *Ozone generation in DC-energized electrostatic precipitators.* IEEE Transactions on Industry Applications, 1992. **28**(3): p. 504-512.
14. Kettleson, E.M., et al., *Airborne Virus Capture and Inactivation by an Electrostatic Particle Collector.* Environmental Science & Technology, 2009. **43**(15): p. 5940-5946.
15. Jiang, S.Y., A. Ma, and S. Ramachandran, *Plant-based release system of negative air ions and its application on particulate matter removal.* Indoor air, 2021. **31**(2): p. 574-586.
16. Suwardi, A., et al., *The efficacy of plant-based ionizers in removing aerosol for COVID-19 mitigation.* Research, 2021. **2021**.
17. Lin, Q., et al., *Sanitizing agents for virus inactivation and disinfection.* VIEW, 2020. **1**(2): p. e16.
18. Mai-Prochnow, A., et al., *Pseudomonas aeruginosa Biofilm Response and Resistance to Cold Atmospheric Pressure Plasma Is Linked to the Redox-Active Molecule Phenazine.* PLOS ONE, 2015. **10**(6): p. e0130373.
19. Wu, Y., et al., *MS2 Virus Inactivation by Atmospheric-Pressure Cold Plasma Using Different Gas Carriers and Power Levels.* Applied and Environmental Microbiology, 2015. **81**(3): p. 996-1002.
20. Hojnik, N., et al., *Effective Fungal Spore Inactivation with an Environmentally Friendly Approach Based on Atmospheric Pressure Air Plasma.* Environmental Science & Technology, 2019. **53**(4): p. 1893-1904.
21. Liao, X., et al., *Combating Staphylococcus aureus and its methicillin resistance gene (mecA) with cold plasma.* Science of The Total Environment, 2018. **645**: p. 1287-1295.
22. Svarnas, P., et al., *Sanitary effect of FE-DBD cold plasma in ambient air on sewage biosolids.* Science of The Total Environment, 2020. **705**: p. 135940.
23. Patange, A., et al., *Assessment of the disinfection capacity and eco-toxicological impact of atmospheric cold plasma for treatment of food industry effluents.* Science of The Total Environment, 2018. **631-632**: p. 298-307.

24. Nwabor, O.F., et al., *A Cold Plasma Technology for Ensuring the Microbiological Safety and Quality of Foods.* Food Engineering Reviews, 2022, 14, 535–554.
25. Mendes-Oliveira, G., et al., *Modeling the inactivation of Bacillus subtilis spores during cold plasma sterilization.* Innovative Food Science & Emerging Technologies, 2019. **52**: p. 334-342.
26. Sakudo, A., T. Misawa, and Y. Yagyu, *Chapter 10 - Equipment design for cold plasma disinfection of food products*, in *Advances in Cold Plasma Applications for Food Safety and Preservation*, D. Bermudez-Aguirre, Editor. 2020, Academic Press. p. 289-307.
27. Terrier, O., et al., *Cold oxygen plasma technology efficiency against different airborne respiratory viruses.* Journal of Clinical Virology, 2009. **45**(2): p. 119-124.
28. Filipić, A., et al., *Cold plasma, a new hope in the field of virus inactivation.* Trends in Biotechnology, 2020. **38**(11): p. 1278-1291.
29. Bourke, P., et al., *The potential of cold plasma for safe and sustainable food production.* Trends in biotechnology, 2018. **36**(6): p. 615-626.
30. Katsigiannis, A.S., D.L. Bayliss, and J.L. Walsh, *Cold plasma for the disinfection of industrial food-contact surfaces: An overview of current status and opportunities.* Comprehensive Reviews in Food Science and Food Safety, 2022. **21**(2): p. 1086-1124.
31. Mirpour, S., et al., *Cold atmospheric plasma as an effective method to treat diabetic foot ulcers: A randomized clinical trial.* Scientific Reports, 2020. **10**(1): p. 1-9.
32. Klämpfl, T.G., et al., *Cold atmospheric air plasma sterilization against spores and other microorganisms of clinical interest.* Applied and environmental microbiology, 2012. **78**(15): p. 5077-5082.
33. Donaghy, J.A., et al., *Relationship of sanitizers, disinfectants, and cleaning agents with antimicrobial resistance.* Journal of Food Protection, 2019. **82**(5): p. 889-902.
34. K S Narayanan, S.S., et al., *Disinfection and Electrostatic Recovery of N95 Respirators by Corona Discharge for Safe Reuse.* Environmental Science & Technology, 2021. **55**(22): p. 15351-15360.
35. Zimmermann, J.L., et al., *Test for bacterial resistance build-up against plasma treatment.* New Journal of Physics, 2012. **14**(7): p. 073037.
36. Suwardi, A., et al., *The Efficacy of Plant-Based Ionizers in Removing Aerosol for COVID-19 Mitigation.* Research (Wash D C), 2021. **2021**: p. 2173642.
37. Ludwig-Begall, L.F., et al., *"Don, doff, discard" to "don, doff, decontaminate"—FFR and mask integrity and inactivation of a SARS-CoV-2 surrogate and a norovirus following multiple vaporised hydrogen peroxide-, ultraviolet germicidal irradiation-, and dry heat decontaminations.* PLOS ONE, 2021. **16**(5): p. e0251872.
38. Stiefel, P., et al., *Critical aspects of using bacterial cell viability assays with the fluorophores SYTO9 and propidium iodide.* BMC Microbiology, 2015. **15**(1): p. 36.
39. Afshari, A., et al., *Electrostatic precipitators as an indoor air cleaner—A literature review.* Sustainability, 2020. **12**(21): p. 8774.
40. Maillard, J.-Y., *Virus susceptibility to biocides: an understanding.* Reviews and Research in Medical Microbiology, 2001. **12**(2): p. 63-74.
41. Kleinstreuer, C., Z. Zhang, and Z. Li, *Modeling airflow and particle transport/deposition in pulmonary airways.* Respiratory Physiology & Neurobiology, 2008. **163**(1): p. 128-138.
42. Rosenberg, M., N.F. Azevedo, and A. Ivask, *Propidium iodide staining underestimates viability of adherent bacterial cells.* Scientific Reports, 2019. **9**(1): p. 6483.
43. Zhang, H., C. Zhang, and Q. Han, *Mechanisms of bacterial inhibition and tolerance around cold atmospheric plasma.* Applied Microbiology and Biotechnology, 2023. **107**(17): p. 5301-5316.
44. Huang, M., et al., *Differences in cellular damage induced by dielectric barrier discharge plasma between Salmonella Typhimurium and Staphylococcus aureus.* Bioelectrochemistry, 2020. **132**: p. 107445.